engineering proceedings

MDPI

Proceeding Paper

Grid Stability Enhancement Using Machine Learning-Tuned Virtual Synchronous Generator †

Ayabonga Mjekula [1,2,*], Shongwe Thokozani [1] and Peter Olukanmi [1]

[1] Department of Electrical Engineering Technology, University of Johannesburg, Johannesburg 2094, South Africa; tshongwe@uj.ac.za (S.T.); polukanmi@uj.ac.za (P.O.)
[2] TNEI Africa, Cape Town 7530, South Africa
* Correspondence: ayabongamjekula57@gmail.com
† Presented at the 34th Southern African Universities Power Engineering Conference (SAUPEC 2026), Durban, South Africa, 30 June–1 July 2026.

Abstract

The increased penetration of renewable energy sources (RES) in the electrical grid has necessitated the concept of a Virtual Synchronous Generator (VSG) control which is used to make grid-connected power electronic converters behave as synchronous generators. While VSG controls are suitable for supporting the inertia of a microgrid, their use leads to grid instability in the event of a disturbance. This research addresses this limitation by integrating a fully connected Feedforward Neural Network (FCNN) into a VSG control to dynamically adjust the damping coefficient and inertia constant in real time. This approach could enhance system stability by reducing frequency and active power oscillations during grid disturbances, particularly during partial load rejection. To evaluate the effectiveness of the proposed method, a supervised learning-based FCNN was trained on VSG damping behavior under various grid disturbances. The trained model was then implemented in a simulation environment to regulate the VSG parameters dynamically. Simulation results show the neural network-based approach reduces high overshoots at the point of disturbance in active power and frequency oscillations; however, the VSG signal settles faster after the grid disturbance. These findings highlight the potential of machine learning in enhancing the stability of VSG-based microgrids, offering a computationally efficient solution for improving transient response and power-sharing performance.

Keywords: Virtual Synchronous Generator (VSG); fully connected neural network controller (FCNN); grid forming (GFM); grid following (GFL)

1. Introduction

The global initiative to decarbonize electrical energy is advancing rapidly. The inquiries regarding energy transition encompass various dimensions: prospective power costs, industrial competitiveness, technological obstacles, and the correlation between energy transition and economic competitiveness. Considering factors such as energy insecurity and climate change, energy transition has become essential [1]. According to [2] countries such as Iceland, Brazil, Costa Rica, and Canada are almost 100 percent renewable, with the majority of their renewable generation being on hydropower plants. The push for Variable Renewable Energy (VES) such as wind and photovoltaic systems has been prevalent in countries like Germany, Denmark, and Ireland. In power systems, stability for a specific starting operating condition signifies that the system will return to its operational equilibrium state following minor perturbations [3]. The notion of robustness in power

Check for updates

Academic Editor: Akshay Kumar Saha

Published: 13 May 2026

Copyright: © 2026 by the authors. Licensee MDPI, Basel, Switzerland. This article is an open access article distributed under the terms and conditions of the Creative Commons Attribution (CC BY) license.

systems extends beyond mere stability. To be strong and resilient, the electric grid must withstand minor disturbances as well as significant equipment failures, human-induced attacks, and natural calamities [3].

This shift to Inverter-Based Resources (IBR) will cause substantial alterations in the structure and operational dynamics of electrical power networks, resulting in considerable stability challenges due to the intrinsic disparities between the dynamics of inverters and synchronous generators [4,5]. The inverters used in renewable integration can be subdivided into two categories, grid forming (GFM) and grid following (GFL) [4]. GFL inverters are inverters that modulate their power output by assessing the phase angle of the grid voltage through a phase-locked loop (PLL). Consequently, they just adhere to the grid angle/frequency and do not actively regulate their frequency output [6]. Nonetheless, the PLL adversely impacts system stability, particularly when the grid is weak due to significant grid impedance. This issue is expected to occur with increasing frequency and complexity globally as synchronous generators are progressively substituted with inverter-based resources (IBRs). As a result, recent years have seen a focus on grid-forming inverters due to their synchronous-generator-like nature [7].

GFM inverters function as voltage sources or frequency regulators to enhance grid stability in IBRs [8]. Grid-forming inverter-based distributed generators (DGs) represent potential energy sources in electric power systems with rotating mass [9]. They enhance environmental cleanliness, reduce energy production costs and power losses, and provide ancillary services for the grid, including reactive power assistance and active filtering [7]. Various publications have focused on the problem of grid stability when GFL and GFM inverters are involved. Grid resilience is the ability to adapt and ride through a disturbance [3]. Grid robustness is the ability to maintain network functionality under optimum conditions [3]. GFL inverters primarily have robust properties, and this will cause instability as more IBRs are integrated into the electrical network [7]. A GFM offers the qualities of a robust and resilient grid; this is shown in the GFM inverter's ability to handle dynamic load changes and transient conditions through active power, frequency, reactive power and voltage controllers [3,7].

Recent innovations have focused on improving the stability and control of grid-forming inverters [6]. One major development is the integration of machine learning [10]. This technology helps improve how grid-forming inverters respond to changes in the grid [5,10].

In addition, optimization algorithms have been used to design better controllers [11]. These improved controllers make grid-forming inverters more effective at supporting grid stability [11]. In [11], Particle Swarm Optimization (PSO) is used as an optimization algorithm to improve the input constraints related to alternating virtual inertia and damping factors in a Virtual Synchronous Generator (VSG) [11]. In turn, the optimized constraints result in reduced reactive power discrepancies, frequency deviations during transient conditions, enhanced small-signal stability, and mitigation of voltage drops in between busses [11].

In comparison to the inertia-based VSG and droop-based controller, the PSO controller showed more efficient results in fixed based conditions [11]. In [12], the bridge in grid resilience and grid robustness is crossed by implementing a VSG controller that uses a Fuzzy Logic Controller and PSO. The FLC dynamically adjusts the virtual inertia and damping factor of the VSG controller to reduce frequency oscillations during a disturbance [12]. The PSO optimizes the Fly Wheel Energy Storage System power reference commands in order to ensure there are not any overshoots [12].

However, the FLCs still lack grid resilience and adaptability, as the FLC rules for the VSG are framed [12]. The bang-bang control strategy offers an alternative dynamic

response [13]. The bang-bang controller implements a threshold control logic that switches the inertia of the VSG based off of the rate of frequency change (RoCoF) [13]. However, the bang-bang controller lacks the complexity to map out the complex relationship between inertia and frequency in unforeseen operating conditions [13].

In order to improve simulation parameters under dynamic conditions, Deep Neural Network Controller (DNNC) offered an alternative approach [5,14]. By using DNNC, the research aims to mitigate active power oscillations and enhance voltage and frequency stability in microgrids [5]. The DNNC integrated characteristics of a constrained Boltzmann machine and a neural network, employing Lyapunov stability theory [5]. The controller can efficiently attenuate oscillations, enhance frequency stability, and optimize microgrid dynamics [5,9]. The computational complexity of a DNNC encapsulates why an alternative solution is provided, as seen in the literature [15]. PSO techniques lack the generalization capabilities for a transient analysis of an evolving power system [16]. A Multi- Layer Feedforward Neural Network (MLFFNN) is an artificial neural network comprising an input layer, one or more hidden layers, and an output layer [16]. Each layer consists of linked neurons, facilitating unidirectional data flow from input to output [16]. MLFFNNs are predominantly utilized for supervised learning tasks, utilizing the backpropagation technique to reduce the discrepancy between predicted and actual outputs by recurrent weight adjustments of connections [10]. Their ability to model complex nonlinear relationships makes them versatile in many applications. The instance of a VSG where the damping coefficient and inertia constant can be varied to reduce frequency and active power oscillations is a great example [17].

The main contributions of this study are:

(1) To improve the grid stability in VSG control by implementing a fully connected Feedforward neural network to dampen frequency and active power oscillations.
(2) The FCNN controller dynamically maps out the relationship between the damping factor and inertia constant to frequency and active power under different X/R and short circuit ratios.
(3) The FCNN controller response is then compared to the VSG controller under the same grid conditions.

The rest of the article is organized as follows. Section 2 shows how the control loop for active power and reactive power loop works for VSG control. Section 3 details the implementation of a Feedforward Neural Network in tandem with VSG control on a grid-forming inverter, defining the purpose of the damping coefficient and inertia constant in VSG control and how a multi-layered Feedforward Neural Network can train and reduce oscillations in active power and frequency during partial load rejection. Section 4 details the results of the FCNN controller against the VSG controller, with a discussion of results in Section 5, detailing the efficiency of the FCNN and VSG controllers under different grid conditions. The article is then concluded in Section 5.

2. Principle Behind the Primary Loop of the VSG

2.1. Control Architecture

As seen in Figure 1 the inner workings of the VSG consist of a PWM signal, current controller, voltage controller, virtual impedance and primary controller. These architectures work in tandem to regulate the output power and form the PCC voltage [18].

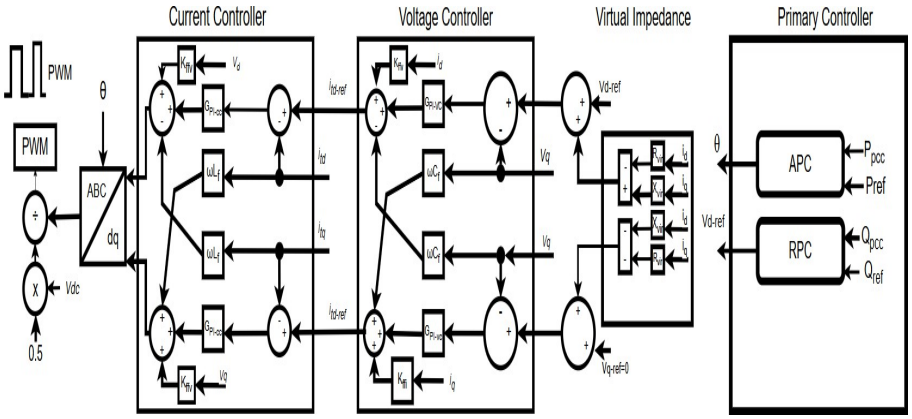


Figure 1. Control Architecture of a VSG.

2.2. Primary Control Loop

The VSG control structure implemented in PSCAD mimics the dynamic behavior of a synchronous machine while interfacing with the grid via a voltage source inverter (VSI) [5,8,18]. The process begins with power calculation, where active and reactive power are computed using voltage and current measurements. These quantities are essential inputs to the Primary VSG Controller, which includes swing equations emulating the inertial and damping characteristics of a real synchronous generator. The following transfer function depicts the control of the active power control loop as seen in Figure 2.

$$P_{ref} - P_{meas} = K_{-P} * \left(\omega_{ref} - \omega_{ind}\right) \quad (1)$$

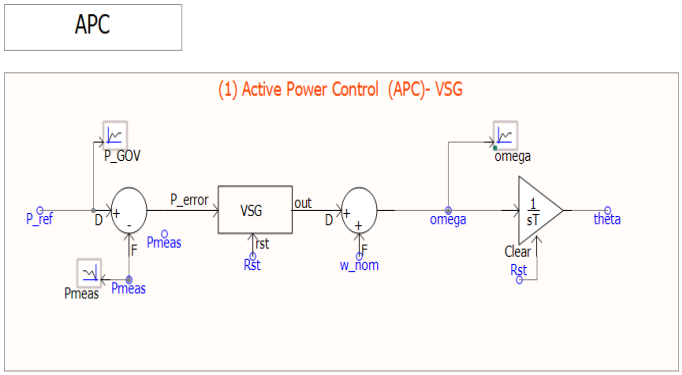


Figure 2. Active Power Control.

The APC function where P_{ref} is the active power reference, P_{meas} is the measured active power output, k_p is the proportional gain constant, the * in Figure 2 represents the multiplication of the proportional gain constant, ω_{ref} is the reference angular speed, and ω_{ind} is the measured internal frequency of the inverter. TheVSG delivers the requisite quantity of active power to the grid. By comparing the reference and measured active power, the controller calculates an error signal. This error signal is then used to alter the VSG's output frequency. A higher error signal leads to a higher output frequency, resulting in increased active power output.

The following transfer function as seen in Figure 3 depicts the control of the reactive power control loop.

$$Q_{ref} - Q_{meas} = K_{-q} * \left(V_{ref} - V_{ind}\right) \quad (2)$$

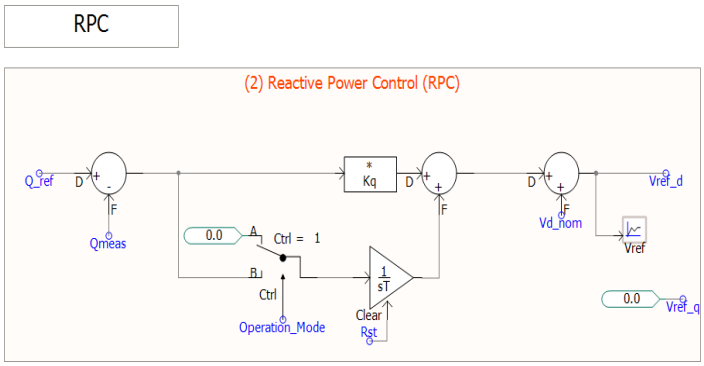


Figure 3. Reactive Power Control.

The following terms refer to Q_{ref} the reference reactive power, Q_{meas} the measured reactive power output, and k_{-q} proportional droop gain constant. V_{ref} refers to the measured voltage setpoint, and V_{ind} refers to the actual internal voltage of the inverter. Similarly, the RPC function guarantees that the VSG sends the required amount of reactive power to the grid. The controller computes an error signal by contrasting the reference and measured reactive power. This error signal is then used to alter the VSG's output voltage magnitude. An elevated error signal produces a greater output voltage magnitude, hence augmenting reactive power production.

2.3. Feedforward Neural Network Controller

As mentioned in Section 1, the VSG leads to grid instability during a grid disturbance, particularly during load rejection. Various methods of damping frequency and active power oscillations during load rejection using a VSG controller have been proposed [11–13]. In this article the VSG controller's primary focus is the APC control loop. Based on the Swing Equation [8], the VSG controller's use is shown in Figure 2.

$$J\frac{d\omega}{dt} = (P_{ref} - P_{meas} - D(\omega_{ref} - \omega_{ind})) \tag{3}$$

where J is the inertia constant, and D is the damping coefficient. The APC mentioned above works with the rate of change of frequency (RoCoF) which is $\frac{d\omega}{dt}$. This RoCoF is determined by a balance between P_{REF} and P_{meas} and D, which is directly proportional to the deviation of the nominal frequency $\left(\omega_{ref} - \omega_{ind}\right)$. J dictates how quickly the frequency can change in response to a power imbalance. A higher J slows down RoCoF by mimicking the behavior of a traditional synchronous machine and providing system stability by preventing abrupt frequency variations [13]. D functions analogously to mechanical friction in a synchronous generator, providing a stabilizing torque that counteracts frequency deviations from the nominal operating point [8]. In the context of a load rejection event where the sudden disconnection of load causes a drop in P_{meas} while P_{ref} remains unchanged, this imbalance results in a net active power that drives the system frequency upward. Inadequate damping under such conditions can lead to sustained oscillations or significant overshoot in frequency. Conversely, a well-tuned D quickly suppresses these oscillations, while sufficient J smooths out the response to prevent an excessive rate of change of frequency (RoCoF). Together, these parameters ensure the VSG can maintain stable frequency output, limit dynamic stress on the inverter, and provide grid-supportive behavior that closely emulates the response of a real synchronous generator. As mentioned in Section 1, various hybrid VSG controllers using D and J components have been attempted [5,11,12,14,15]; in this paper the FCNN controller is used to provide an adaptive solution under different grid conditions to provide grid resiliency and grid stability.

Figure 4 shows the control structure of the FCNN. It consists of a VSG, containing an FCNN controller that generates control signals that are sent to the PWM block, which in turn governs the inverter behavior.

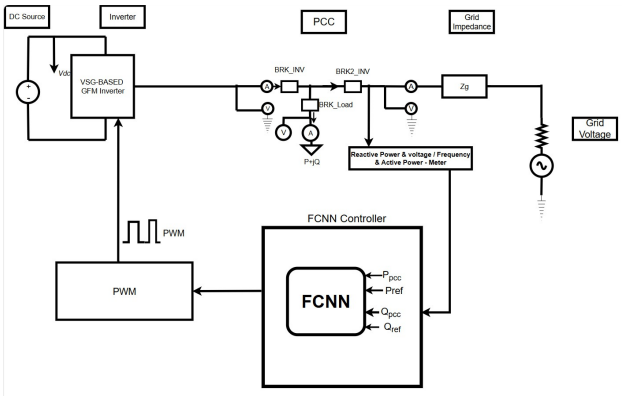


Figure 4. Block diagram of VSG with Neural Network Controller.

2.4. Multi-Layered Feedforward Neural Network

A Multi-layer Feedforward Neural Network (FFNN) is an artificial neural network comprising an input layer, one or more hidden layers, and an output layer [16]. Each layer consists of linked neurons, facilitating unidirectional data flow from input to output [16]. Feedforward Neural Networks (FFNNs) are predominantly utilized for supervised learning tasks, utilizing the backpropagation technique to reduce the discrepancy between predicted and actual outputs by recurrent weight adjustments of connections [16]. Figure 5 illustrates the structure of an FFNN.

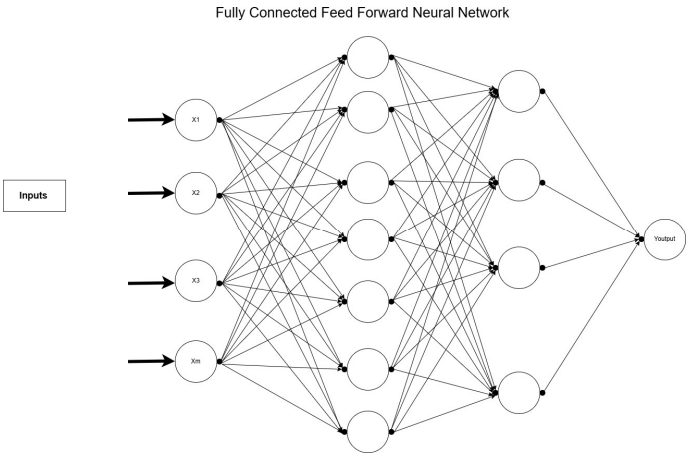


Figure 5. Fully connected Feedforward Neural Network Structure.

The FFNN architecture consists of an input layer and two hidden layers, a drop out layer for regularization, and a linear output layer for regression. It is best suited for static regression models. The model uses a multi-layered perceptron (MLP), and each hidden layer performed a weighted sum of its inputs followed by a nonlinear activation using the Rectified Linear Unit (ReLU), mathematically expressed as:

$$z^l = W^{l-1} + b^l,\ a^l = max\left(0, z^l\right) \tag{4}$$

where W^l and b^l denote the weights and biases of layer l, respectively, and $x^{(l-1)}$ represents the input from the previous layer.

$$a^l = f\left(W^l a^{l-1} + b^l\right) \tag{5}$$

where a^l is the activation layer, W^l is the learned weight matrix and b^l is the bias term. The network's parameters {W, b} are iteratively updated using backpropagation and the Adam optimizer to minimize the mean squared error between predicted and actual dynamic responses.

The final output layer applied a linear activation function:

$$\widehat{y} = W^L x^{(L-1)} + b^L \tag{6}$$

to predict the optimal control actions needed for stabilizing the inverter response. Model training was conducted using the Adam optimizer, which incorporates momentum and adaptive learning rates based on first- and second-moment estimates of the gradients. The gradient of the loss function is illustrated as follows:

$$G_t = \nabla L W_t \tag{7}$$

with L being the loss function with respect to the weights W_t. The mean of the gradient is illustrated as follows.

$$m_t = \beta m_{t-1} + (1 - \beta)\nabla l(W_T) \tag{8}$$

The purpose of this formula is to scale each parameter individually based on recent gradients, which allows adaptive learning rates and smoother convergence. The FFNN was trained to minimize the mean squared error (MSE) loss between predicted control setpoints and actual system targets. By incorporating D and H into the input feature space, the FCNN learns on context-sensitive control policies, enabling it to generate damping-enhanced responses to minimize oscillatory behavior in the VSG's active power and frequency response.

2.5. The FCNN Structure

The FCNN suggested structure is suggested in Figure 5 above. The purpose of the FCNN is for it to be utilized as a data-driven model to learn the complex nonlinear dynamics that influence frequency and active power oscillations in a VSG. Specifically, the FCNN serves as a regression tool that maps key control parameters, such as the damping coefficient and inertia constant, to expected dynamic responses, including deviations in frequency and active power during load rejection. The FCNN architecture as shown in Figure 6 is particularly suited for this application to approximate nonlinear functions.

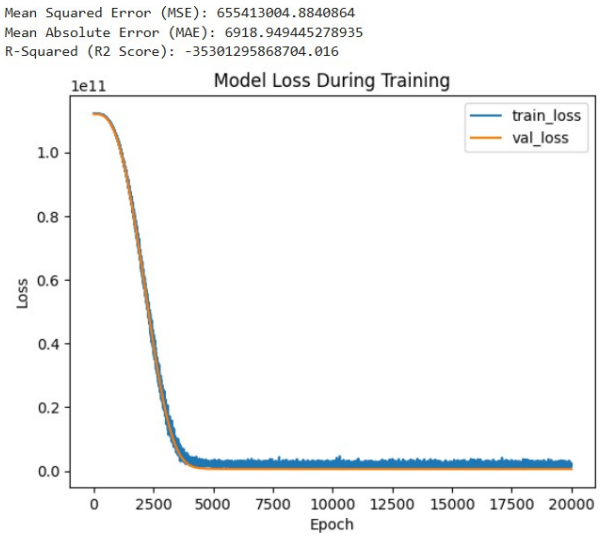


Figure 6. FCNN modelling performances.

3. Results

In this section, a summary of the results is provided. The initial input parameters of the PSCAD simulation are shown in Table 1. Figure 6 exhibits the graphical performance of the FCNN controller, which is then represented numerically by the Mean Absolute Error and Loss Function in Table 2. Table 3 displays the FCNN controller results for the FCNN controller under different grid conditions. Figure 7 is the graphical result for the VSG controller vs. FFNN controller.

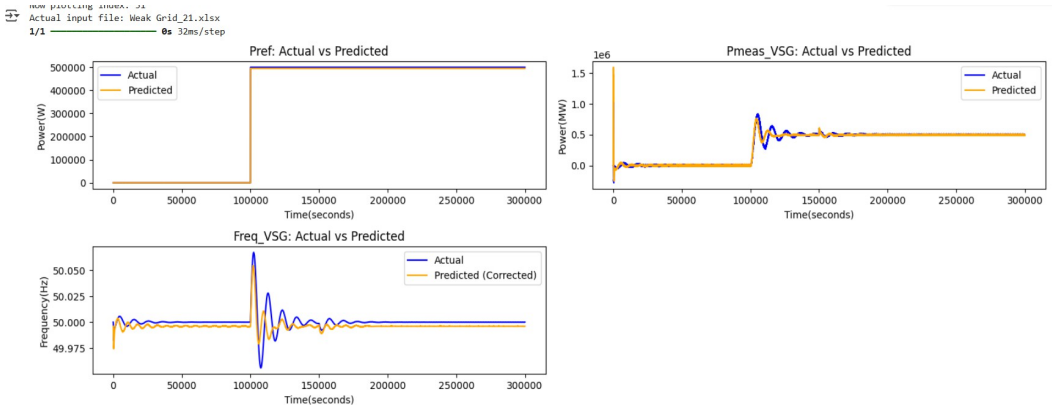


Figure 7. FCNN vs. VSG.

Table 1. Simulation parameters.

Input Grid Parameters	Value	Unit	Description
Vgrid	690	V	Grid Voltage
Fgrid	50	Hz	Grid Frequency
SCR	1.5	-	Worst Case Grid Condition
SCR	3	-	Weak Grid
SCR	8	-	Strong Grid
SCR	14	-	Robust Strong Grid
Srated	1	MVA	Inverter Rated Power
Prated	1	MW	Inverter rated Active Power
Qrated	0	MVar	Inverter Reactive Power
Vdc	1.7	kV	DC bus voltage
Lf	$1.5 \times \epsilon^{0.5}$	H	filter Inductance
Rf	0.01	Ohm	Filter Resistance
Cf	0.002	F	Filter Reactance
MpV SG	$1/3.141 \times \epsilon^{0.6}$	W.s/rad	VSG Damping Coefficient
JV SG	506.6	$W.s^2/rad$	VSG Inertia Constant
kqV SG	$1/5.520 \times \epsilon^{0.5}$	V/Var	VSG Droop Coefficient

https://doi.org/10.3390/engproc2026140010

Table 2. FCNN controller evaluation metric.

Neural Network Model	Mean Absolute Error	Loss Function
FCNN	6918.949	920489586

Table 3. Summary of graphical results for FCNN controller vs. VSG controller.

Type of Grid	SCR	X/R	Performed or Underperformed
Strong Grid 15	11	10	performed
Strong Grid 4	7	14	performed
Strong Grid 18	7	10	performed
Strong Grid 2	7	11	underperformed
Weak Grid 16	6	2	performed
Weak Grid 14	7	2	performed
Weak Grid 18	6	2	performed
Weak Grid 19	5	5	performed
Weak Grid 21	6	6	underperformed

4. Discussions

In this section, the performance of the proposed Feedforward Neural Network FCNN controller is evaluated against the conventional VSG control strategy described in Section 2. The objective is to assess the FCNN's ability to reduce oscillations and accurately capture the complex nonlinear relationships between control inputs and system responses under varying grid conditions, particularly during load rejection. The FCNN is trained on a dataset that includes variations in both the damping coefficient, inertia constant, and grid strength. It is then deployed at the primary control level of the VSG within the PSCAD simulation environment. The FCNN controller is trained on a data set with a varied damping coefficient, inertia constant, and Q-V droop coefficient at the primary controller of the virtual synchronous generator in the PSCAD model. The epochs run an iteration of the Feedforward Neural Network loop. Going through the first layer with the inputs of the damping coefficient, inertia constant, and Q-V droop coefficient, this layer contains a 32-neuron dense layer with 224 parameters; the second dense layer that passes through has 64 neurons and is outputted on the final layer with 2,400,008 neurons. This would then be evaluated in the mean loss error and loss function to assess model performance. Table 2 shows the mean absolute error and loss function performance of the FCNN model. The PSCAD model performs partial active power rejection by injecting reference active power into the inverters at 10 s; this causes an increase in frequency and active power. As seen in Figure 7, at exactly 10,000 time steps there is a spike in frequency and active power after the oscillations in the VSG and FCNN controller signals return to steady-state conditions. The FCNN controller signal compared to the VSG signal shows that the oscillations are identical in response, but the FCNN is more oscillatory in nature than the VSG signal but has less overshoots than the VSG controller. The active power response in the VSG has a higher overshoot than the FCNN controller; however, the FCNN controller has a less stable steady-state signal response than the VSG controller. The reactive power response in the VSG controller and the FCNN are identical; this is because the response of the active power controller is observed and the Q-V droop coefficient is kept stable, but in this instance it is a clear indication of the input and output relationship between the Q-V droop coefficient and the output reactive power, both in the VSG controller and FCNN controller. In evaluating the performance of the FCNN controller against the VSG controller under varying grid

conditions, a clear trend emerges from both the tabulated summary and the waveform responses. Table 3 presents a comparative overview of controller performance across grid strengths with different Short Circuit Ratios (SCR) and X/R values. The FCNN controller consistently performs well under strong grid conditions, specifically in cases with higher SCR and X/R values such as Strong Grid 15 (SCR = 11, X/R = 10), Strong Grid 4 (SCR = 7, X/R = 14), and Strong Grid 18 (SCR = 7, X/R = 10). However, its performance degrades in certain scenarios like Strong Grid 2 (SCR = 7, X/R = 11) and Weak Grid 21 (SCR = 6, X/R = 6), indicating sensitivity to weak grid conditions.

5. Conclusions

This study aimed to enhance grid stability in frequency and active power oscillations by integrating machine learning into Virtual Synchronous Generator (VSG) control. A fully connected Feedforward Neural Network (FCNN) was implemented to dynamically dampen frequency and active power oscillations during partial load rejection. The FCNN successfully learned and mapped the nonlinear relationship between damping factor and inertia constant under varying X/R and short circuit ratios, enabling adaptive parameter tuning. A comparison between the FCNN and the VSG controller then demonstrated that the FCNN-based approach provided less overshoots at the point of disturbance; however, the VSG controller has a faster settling response after the grid disturbance. The FCNN controller, having lower overshoots, shows its potential in enabling the responses of grid-forming inverters under weak grid conditions. Another application of the FCNN controller can be training the FCNN on more weak grid data to improve the stability of VSG control in weak inertia systems. Further applications such as voltage and reactive power stability parameter tuning can be assessed with an FCNN controller. Future research should explore real-time hardware implementation, scalability to multi-inverter systems, and integration with other advanced control strategies such as reinforcement learning to further optimize grid-forming inverter performance.

Author Contributions: Conceptualization, A.M. and S.T.; Methodology, A.M.; Software; A.M.; Validation, A.M. Formal Analysis: A.M.; data curation: A.M.; Writing original draft preparation, A.M.; writing-review and editing; P.O. and S.T.; Supervision; P.O. and S.T. All authors have read and agreed to the published version of the manuscript.

Funding: This research received no external funding.

Informed Consent Statement: Not applicable.

Data Availability Statement: Please email: ayabongamjekula57@gmail.com for data availability.

Conflicts of Interest: Author Ayabonga Mjekula was employed by the company TNEI Africa. The remaining authors declare that the research was conducted in the absence of any commercial or financial relationships that could be construed as a potential conflict of interest.

References

1. Mirmohammad, M.; Azad, S.P. Control and stability of grid-forming inverters: A comprehensive review. *Energies* **2024**, *17*, 3186. [CrossRef]
2. Kroposki, B.; Johnson, B.; Zhang, Y.; Gevorgian, V.; Denholm, P.; Hodge, B.-M.; Hannegan, B. Achieving a 100% renewable grid: Operating electric power systems with extremely high levels of variable renewable energy. *IEEE Power Energy Mag.* **2017**, *15*, 61–73. [CrossRef]
3. Arghandeh, R.; Von Meier, A.; Mehrmanesh, L.; Mili, L. On the definition of cyber-physical resilience in power systems. *Renew. Sustain. Energy Rev.* **2016**, *58*, 1060–1069. [CrossRef]
4. Gu, Y.; Green, T.C. Power system stability with a high penetration of inverter-based resources. *Proc. IEEE* **2022**, *111*, 832–853. [CrossRef]

5. Ghodsi, M.R.; Tavakoli, A.; Samanfar, A. Microgrid stability improvement using a deep neural network controller based vsg. *Int. Trans. Electr. Energy Syst.* **2022**, *2022*, 7539173. [CrossRef]
6. Pattabiraman, D.; Lasseter, R.H.; Jahns, T.M. Comparison of grid following and grid forming control for a high inverter penetration power system. In *2018 IEEE Power & Energy Society General Meeting (PESGM)*; IEEE: New York, NY, USA, 2018; pp. 1–5.
7. Li, Y.; Gu, Y.; Green, T.C. Revisiting grid-forming and grid- following inverters: A duality theory. *IEEE Trans. Power Syst.* **2022**, *37*, 4541–4554. [CrossRef]
8. Rathnayake, D.B.; Akrami, M.; Phurailatpam, C.; Me, S.P.; Hadavi, S.; Jayasinghe, G.; Zabihi, S.; Bahrani, B. Grid forming inverter modeling, control, and applications. *IEEE Access* **2021**, *9*, 114781–114807. [CrossRef]
9. Ulbig, A.; Borsche, T.S.; Andersson, G. Impact of low rotational inertia on power system stability and operation. *IFAC Proc. Vol.* **2014**, *47*, 7290–7297. [CrossRef]
10. Danish, M.S.S. *Unified Vision for a Sustainable Future*; Springer: Berlin/Heidelberg, Germany, 2024.
11. Rathore, B.; Chakrabarti, S.; Anand, S. Frequency response improvement in microgrid using optimized vsg control. In *2016 National Power Systems Conference (NPSC)*; IEEE: New York, NY, USA, 2016; pp. 1–6.
12. Kumar, A.W.; Mufti, M.U.D.; Zargar, M.Y. Fuzzy based virtual inertia emulation in a multi-area wind penetrated power system using adaptive predictive control-based flywheel storage. *Sustain. Energy Technol. Assess.* **2022**, *53*, 102515. [CrossRef]
13. Li, J.; Wen, B.; Wang, H. Adaptive virtual inertia control strategy of vsg for micro-grid based on improved bang-bang control strategy. *IEEE Access* **2019**, *7*, 39509–39514. [CrossRef]
14. Im, M.S.; Dasari, V.R. Computational complexity reduction of deep neural networks. *arXiv* **2022**, arXiv:2207.14620. [CrossRef]
15. Yao, J.; Luo, X.; Li, F.; Li, J.; Dou, J.; Luo, H. Research on hybrid strategy particle swarm optimization algorithm and its applications. *Sci. Rep.* **2024**, *14*, 24928. [CrossRef] [PubMed]
16. Svozil, D.; Kvasnicka, V.; Pospichal, J. Introduction to multi-layer feed-forward neural networks. *Chemom. Intell. Lab. Syst.* **1997**, *39*, 43–62. [CrossRef]
17. Lamnatou, C.; Cristofari, C.; Chemisana, D. Renewable energy sources as a catalyst for energy transition: Technological innovations and an example of the energy transition in France. *Renew. Energy* **2024**, *221*, 119600. [CrossRef]
18. Mohammed, N.; Udawatte, H.; Zhou, W.; Hill, D.J.; Bahrani, B. Grid-forming inverters: A comparative study of different control strategies in frequency and time domains. *IEEE Open J. Ind. Electron. Soc.* **2024**, *5*, 185–214. [CrossRef]

Disclaimer/Publisher's Note: The statements, opinions and data contained in all publications are solely those of the individual author(s) and contributor(s) and not of MDPI and/or the editor(s). MDPI and/or the editor(s) disclaim responsibility for any injury to people or property resulting from any ideas, methods, instructions or products referred to in the content.